Acta Geodyn. Geomater., Vol. 9, No. 4 (168), 427–433, 2012

COMPARISON OF GPS SLANT WET DELAYS ACQUIRED BY DIFFERENT TECHNIQUES

Michal KAČMAŘÍK [1] *, Jan DOUŠA [2] and Jan ZAPLETAL [3]

[1] *Institute of Geoinformatics, Faculty of Mining and Geology, VŠB–Technical University of Ostrava, 17. listopadu 15, 708 00 Ostrava Poruba, Czech Republic*
[2] *Research Institute of Geodesy, Topography and Cartography, Geodetic Observatory Pecný, 251 65 Ondřejov 244, Czech Republic*
[3] *Department of Applied Mathematics, Faculty of Electrical Engineering and Computer Science, VŠB–Technical University of Ostrava, 17. listopadu 15, 708 00 Ostrava Poruba, Czech Republic*
**Corresponding author's e-mail:* michal.kacmarik@vsb.cz

(*Received* March 2012*, accepted* May 2012)

ABSTRACT
This paper discusses the quality of slant wet delays (SWD) computed from GPS measurements. The SWDs are generally used as input data for GPS tomography, which allows the three-dimensional reconstruction of water vapour distribution in the atmosphere. The research presented is based on a comparison of slant wet delays acquired by different strategies based on double-differenced Global Positioning System (GPS) data. The GPS-derived SWDs were compared with those directly measured by a water vapour radiometer (WVR). The best results from the applied GPS strategies were achieved by a simple mapping of GPS-derived zenith total delays into SWD without adding horizontal gradients or post-fit residuals.

KEYWORDS: GPS tomography, slant wet delay, water vapour radiometer, post-fit residual, multipath

INTRODUCTION

It has been shown many times that the GPS system is useful for the estimation of troposphere parameters - the approach called GPS meteorology (Bevis et al., 1992; Duan et al., 1996). In a classic GPS meteorology scenario, we calculate the zenith total delay (ZTD) and potentially convert it into precipitable water vapour, PWV (Bevis et al., 1994). The ZTD or PWV is, however, not able to provide information about the vertical distribution of water vapour or its dense three-dimensional field. This information can be obtained by a GPS tomography technique dividing the space above a network of GPS receivers into a system of voxels, reconstructing water vapour in each voxel. The primary input data for the GPS tomography used by most tomography projects are slant wet delays (SWD), which are either zero-differenced (Flores et al., 2001; Noguchi et al., 2001; Champollion et al., 2004; Gradinarsky and Jarlemark, 2004; Bender et al., 2011) or double-differenced (Troller et al., 2006). The quality of GPS-derived SWD strongly influences the tomography results and it is therefore important to assess the best strategy. Some tomography projects use horizontal gradients or post-fit residuals added to raw GPS slant wet delays to reconstruct the anisotropic part of the atmosphere (Flores et al., 2001; Noguchi et al., 2001; Gradinarsky and Jarlemark, 2004; Bender et al., 2011), but other authors (Gradinarsky and Jarlemark, 2004; Nilsson et al., 2005) are sceptical of such a process. In this paper, the various SWDs were compared with water vapour radiometer (WVR) measurements to evaluate the real impact of horizontal gradients and post-fit residuals with or without multipath corrections. While Bender et al. (2008) presented a comparison of SWD from GPS and radiometer data based on Precise Point Positioning (Zumberge et al., 1997) processing, our study is based on the double-differencing technique and reconstructed zero-difference post-fit residuals (Alber et al., 2000).

The first section provides details about the GPS processing, the second section presents the calculation of SWDs, the third section compares SWDs achieved by various GPS strategies with WVR, and the final section gives the conclusion.

GPS DATA PROCESSING

In this study, the Bernese GPS Software 5.0 (Dach et al., 2007) was used for the ZTD computation. The basic characteristics of GPS processing are summarized in Table 1. A network of 28 GPS reference stations was used with nine stations situated in the Czech Republic and all others over a larger European territory. The station with the lowest elevation is situated 45 m above sea level, and the station with the highest elevation is 951 m above sea level. In general, for GPS tomography water vapour reconstruction, it is helpful to provide SWDs derived from observations of all available Global Navigation Satellite Systems (GNSS), i.e., in addition to GPS NAVSTAR, almost the entire GLONASS constellation and the first Galileo satellites in the near

Table 1 Basic characteristics of ZTD processing in Bernese GPS SW.

Ephemerides, Satellite clocks	IGS Rapid
Sampling rate	180 s
Elevation cut-off angle	3°
Mapping function	Niell
Phase Centre Correction	IGS model applied
Ocean Loading	Applied
Observables	Double differences
ZTD, gradient estimation interval	30 min
Pole information	IGS rapid
Differential Code Bias information	CODE 30-day solution

future. However, only data from the GPS NAVSTAR were used in this study because we focus mainly on a comparison of various SWD strategies with respect to WVR. The WVR was capable of pointing to GPS satellites only, and only some stations in the network observed the GLONASS system. Finally, adding GLONASS observations could add additional systematic errors into our solutions based, for example, from the phase centre variation model.

The reference GNSS site GOPE is the principal station for this study because it is located only a few meters from the Radiometrics TP/WVP-3000 (No. 3025) water vapour radiometer on the roof of the main building. This WVR has only GPS NAVSTAR antenna, thus it is not able to track GLONASS satellites. Although WVR has also a full sky scanning mode, a GPS pointing mode was used in order to collect as many as direct observation to GPS satellites for comparisons. The TP/WVP-3000 WVR at GOPE site (installed in 2006) has the capability of tracking 5 K-band (22-30 GHz) and 7 V-band (51-59 GHz) microwave channels. It requires, however, the clear sky without any interference. Since mobile operators' transmission towers using 24 GHz frequency for inter-tower communications are located in the east-west direction, a specific metallic shield was installed. Additionally, the WVR provides a rain detection flag, because such measurements are affected, and data from these flagged periods were eliminated from the comparison. The WVR beam widths range is 2.5 and 5-6° for V-band and K-band, respectively. An elevation angle of WVR measurements was selected as 10 ° (considering an installation on a roof partly avoiding a ground radiation) since V-band is important for the estimation of humidity. By analysing the microwave spectrum emitted by the atmospheric water molecules, the WVR provides SWDs suitable observations for independent comparisons with those derived from the GPS measurements.

GNSS data from a total of 39 days were processed during 2011. These data were separated into four 7-11 day periods and processed independently (January 19 – 27, February 17 – 27, June 24 – July 3, October 17 – 27). These periods were selected to evaluate the results gathered under different weather conditions and using data from more seasons. The PWV values ranged between 2 and 28 millimetres during the selected days.

We evaluated the quality of our achieved ZTD solutions through their comparison with ZTDs from other sources. First, we compared our solutions to ZTDs with an hour resolution from the Geodetic Observatory Pecny analysis centre (GOP) final daily solutions contributing to the EUREF Permanent Network (EPN) based on double-differenced observations processed with Bernese GPS software. Second, we compared them with the final IGS ZTD solutions downloaded from CDDIS (Crustal Dynamics Data Information System) based on the Precise Point Positioning technique and providing a five-minute resolution. It should be noted that until GPS week 1631, the IGS final tropospheric product was produced by JPL using GIPSY/OASIS software (Sever, 2010) and, from 1632 (inclusive), by USNO using Bernese GPS software (Byram, 2011). Because all three sources use different ZTD time intervals, only those ZTDs from identical epochs were compared. The results are shown in Table 2, and they generally prove the expected quality of the agreement between various post-processing ZTD results, which can be characterized with a standard deviation of 2-3 mm. The larger biases in June/July and in October with respect to the CDDIS ZTDs could be caused by the change of the IGS final ZTD product provider (Byram, 2011). Higher standard deviations (SDEVs) during the summer and autumn periods are related to the seasonal trend of water vapour development, with much higher values and variability during the warmer part of year.

SLANT WET DELAY COMPUTATION

The zenith total delay can be separated into a hydrostatic part (Zenith Hydrostatic Delay, ZHD), related to the atmospheric pressure, and a wet part (Zenith Wet Delay, ZWD) which is dependent on the water vapour in the troposphere. Using the Saastamoinen model (Saastamoinen, 1973) and values of atmospheric pressure and temperature precisely measured at GOPE, the extraction of ZWD from ZTD in 30-minute intervals was performed.

Slant Wet Delay can then be computed for each observation between a receiver and a satellite using

Table 2 Comparison of ZTD from different sources.

Time Period	Presented – GOPE EPN		Presented – IGS PPP		IGS PPP – GOPE EPN	
	Bias (mm)	SDEV (mm)	Bias (mm)	SDEV (mm)	Bias (mm)	SDEV (mm)
January	1.29	1.49	0.9	1.92	0.36	1.88
February	1.11	1.32	0.27	1.73	0.82	1.9
June - July	-0.55	2.98	-2.15	3.01	1.56	2.95
October	0.85	2.42	-1.1	3.22	1.84	2.74

the formula:

$$SWD(\varepsilon,\theta) = m(\varepsilon)*(ZWD + \cot g\, \varepsilon(G_N*\cos\theta + G_E*\sin\theta)) + R,$$

where ε, θ is the elevation and azimuth angle of a satellite, m(ε) is a mapping function giving the relation between the zenith tropospheric wet value to the wet path delay in a direction to a particular satellite, GN and GE are estimated north and east horizontal gradients, respectively, and R represents a post-fit residual of the ZTD model with respect to the observation. The estimated part of the ZTD and horizontal tropospheric gradients are assumed to be a wet part of the total tropospheric delay only. The reason is that the currently official Bernese GPS software (v5.0) doesn't support the correct separation of hydrostatic and wet delays as well as horizontal tropospheric gradients, based e.g. on external information from the Vienna mapping function – VMF1 (Boehm et al., 2006; Boehm and Schuh, 2007) both derived applying data from a numerical weather prediction model.

Horizontal tropospheric gradients and line-of-sight post-fit residuals could give additional information about the anisotropic distribution of water vapour around a station, thus theoretically providing results closer to the real state of the atmosphere. In this study, four types of SWDs were evaluated:

1. SWD1 computed only from ZWD,
2. SWD2 computed from ZWD and horizontal gradients,
3. SWD3 computed from ZWD, horizontal gradients and post-fit residuals,
4. SWD4 computed from ZWD, horizontal gradients and post-fit residuals after correction for the multipath.

The Niell mapping function (Niell, 1996) was used in this study. The horizontal gradients were estimated during the GPS data processing in the same time interval as ZTD. Because the double-differencing was applied for the ZTD estimation, the resulting double-differenced residuals had to be transformed into zero-differenced residuals, which was sukcessfully done using the technique described by Alber et al. (2000). It is important to keep in mind that this process is built on specific zero mean assumptions, which can cause significant systematic errors, as proved by Elosegui and Davis (2003), and therefore does not represent an ideal solution. The resulting line-of-sight (zero-differenced) residuals should mainly contain the anisotropic part of the wet delay, multipath and unmodeled antenna phase centre variations.

The stacking technique described in Shoji et al. (2004) was applied to reduce the multipath from the residuals. Stacking maps were constructed with a resolution of 1°. Each bin of those maps represents the mean residual values in particular azimuth/elevation direction, computed from all available residuals from a selected time period. The systematic values in the residuals are considered to be caused mainly by the multipath effect, but potentially also by the errors in the phase centre variation model. The stacking maps were constructed from 11 days of GPS data corresponding to the selected periods. We also tried an optimal interval of 7 days, as proposed by Bender et al. (2008), but it led to worse results in our case.

Figures 1 and 2 show the multipath maps constructed for the January and June/July periods. The elevation cut-off angle was set to 5°. It is clear that the multipath values during the summer period are mainly at lower elevations higher, more so than during the winter period. This situation is quite surprising, and it may have been caused by the inability of the used mapping function and the whole tropospheric modelling to provide fine results at lower elevation angles when the amount of water vapour in the atmosphere is larger; but this is only an assumption, and extensive work would be necessary to verify the situation.

COMPARISON OF RESULTS FROM GPS AND RADIOMETER MEASUREMENTS

All types of computed SWDs were compared with the WVR measurements. Statistical processing was performed using all SWD pairs from the GPS and radiometer, which were generated from observations at identical epochs to a single GPS satellite. Approximately 1,000 identical pairs were created for each day.

Table 3 shows the results for the SWD values mapped back into the zenith direction and thus representing the ZWDs. Comparing the biases from the various time periods, there is a significant difference between the first two periods and the

Table 3 Comparison of slant wet delays from GPS and WVR mapped to zenith direction for particular time periods. SDEV represents standard deviation and RMSE root-mean square error.

Period	Statistical parameter [mm]	ZWD1 - WVR	ZWD2 - WVR	ZWD3 - WVR	ZWD4 - WVR	Number of pairs	Mean ZWD1 value [mm]
January	Bias	-1.18	-1.17	-1.12	-1.14	6 974	37.5
	SDEV	4.43	4.47	5.61	5.31		
	RMSE	4.58	4.62	5.72	5.51		
February	Bias	-2.42	-2.42	-2.45	-2.48	10 593	36.4
	SDEV	4.46	4.49	5.68	5.53		
	RMSE	5.08	5.1	6.18	6.06		
June - July	Bias	-14.59	-14.57	-14.56	-14.59	9 534	103.18
	SDEV	7.66	7.75	9.46	9.09		
	RMSE	16.48	16.5	17.36	17.19		
October	Bias	-13.47	-13.47	-13.38	-13.47	9 744	69.93
	SDEV	5.19	5.21	6.63	6.20		
	RMSE	14.44	14.44	14.93	14.83		

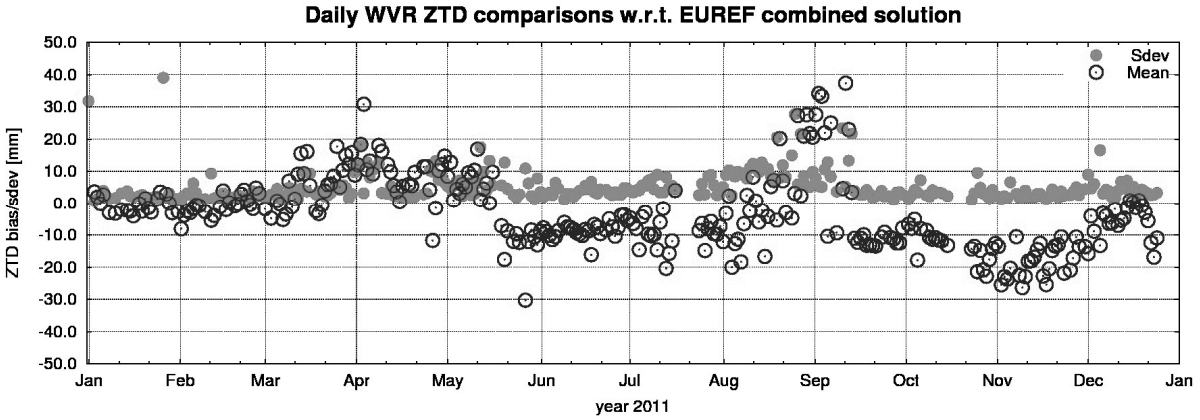

Fig. 3 Comparison of GPS and WVR ZTD measurements for 2011, station GOPE.

others. The quality of the WVR measurements during 2011 varied widely, as shown in Figure 3, which presents a comparison of the ZTD values from GPS and WVR. After January and February, when the results were in a good agreement, the following months show mainly unstable and biased results. The situation did not improve, even after recalibration on May 19th and September 13th. Nevertheless, the main goal of this study is to compare the various types of SWDs from GPS measurements, and thus, the figure mainly helped us to identify the periods with either good or poor quality WVR measurements. The existing biases between GPS and WVR do not limit our comparisons (aimed for the standard deviation); however, the unstable WVR quality, indicated by the large standard deviations, negatively influences them (we cannot trust WVR as we hoped). This situation also shows the variable stability of a long-term operative run of the WVR at Geodetic Observatory Pecny.

According to Table 3, the contribution of horizontal gradients to the SWD is very small under particular atmospheric conditions. The Table shows a potentially positive influence on bias, but also a small negative impact on the standard deviation. The table also shows that including the gradients in the SWD will not generally result in any advantage and would possibly make sense only in specific atmospheric situations with an evident and clear anisotropy in the atmosphere (e.g., front passage).

Adding the post-fit residuals increased the standard deviation of SWD by approximately 1.1 – 1.7 mm for values mapped to the zenith direction. For use in GPS tomography, the positive impact of a slightly smaller bias between GPS and VWR with added residuals would not compensate the larger SDEV, which can result in significant problems during the tomographic reconstructions. The indication is that the post-fit residuals do not only contain information about the anisotropic part of the atmosphere but also other source errors.

The situation improves if the multipath stacking maps are applied, but the SDEV still stays approximately 0.9 – 1.4 mm larger than in the raw GPS data case. These results of such a small positive impact from applying multipath maps are very similar to the results by Bender et al. (2008), although the PPP technique was used for the determination of ZTD

Table 4 Comparison of slant wet delays from GPS and WVR for the January period, all bias and SDEV values in [mm].

Elevation angle [°]	Bias SWD1 - WVR	Bias SWD2 - WVR	Bias SWD3 - WVR	Bias SWD4 - WVR	SDEV SWD1 - WVR	SDEV SWD2 - WVR	SDEV SWD3 - WVR	SDEV SWD4 - WVR	Number of pairs
10 - 20	-7.63	-7.62	-7.38	-7.21	11.27	11.3	13.23	13.09	916
20 - 30	-5.71	-5.71	-5.96	-5.81	7.69	7.72	10	9.5	1 329
30 - 40	-1.96	-1.93	-1.64	-1.82	5.47	5.53	7.63	7.26	1 227
40 - 60	-0.7	-0.66	-0.62	-0.75	5.99	6.05	7.95	7.59	1 822
60 - 90	-0.5	-0.5	-0.41	-0.39	6.32	6.38	7.75	7.49	1 680

Table 5 Comparison of slant wet delays from GPS and WVR for the February period, all bias and SDEV values in [mm].

Elevation angle [°]	Bias SWD1 - WVR	Bias SWD2 - WVR	Bias SWD3 - WVR	Bias SWD4 - WVR	SDEV SWD1 - WVR	SDEV SWD2 - WVR	SDEV SWD3 - WVR	SDEV SWD4 - WVR	Number of pairs
10 - 20	-7.97	-7.97	-7.8	-7.74	9.64	9.64	11.98	11.96	1 643
20 - 30	-6.16	-6.14	-6.49	-6.38	7.61	7.62	9.91	9.54	1 953
30 - 40	-4.1	-4.08	-3.82	-4.26	6.74	6.76	8.76	8.53	1 837
40 - 60	-2.93	-2.92	-3.02	-3.06	6.71	6.75	8.53	8.31	2 643
60 - 90	-2.91	-2.91	-3.02	-2.94	6.15	6.19	7.72	7.54	2 517

Table 6 Comparison of slant wet delays from GPS and WVR for the June-July period, all bias and SDEV values in [mm].

Elevation angle [°]	Bias SWD1 - WVR	Bias SWD2 - WVR	Bias SWD3 - WVR	Bias SWD4 - WVR	SDEV SWD1 - WVR	SDEV SWD2 - WVR	SDEV SWD3 - WVR	SDEV SWD4 - WVR	Number of pairs
10 - 20	-49.68	-49.63	-49.19	-49.36	26.89	27.06	32.09	31.13	970
20 - 30	-34.9	-34.91	-34.61	-34.69	17.98	18.09	22.17	21.19	1 912
30 - 40	-24.43	-24.39	-24.24	-24.67	13.89	14.05	17.15	16.55	1 700
40 - 60	-18.47	-18.46	-18.62	-18.43	10.28	10.39	12.59	12.05	2 547
60 - 90	-16.55	-16.61	-16.71	-16.7	8.07	8.2	10.19	9.73	2 405

Table 7 Comparison of slant wet delays from GPS and WVR for the October period, all bias and SDEV values in [mm].

Elevation angle [°]	Bias SWD1 - WVR	Bias SWD2 - WVR	Bias SWD3 - WVR	Bias SWD4 - WVR	SDEV SWD1 - WVR	SDEV SWD2 - WVR	SDEV SWD3 - WVR	SDEV SWD4 - WVR	Number of pairs
10 - 20	-38.99	-39.01	-38.33	-38.70	16.24	16.30	19.21	18.26	934
20 - 30	-28.45	-28.44	-28.27	-28.55	10.56	10.60	13.97	12.59	1 968
30 - 40	-20.99	-21.00	-20.28	-21.10	7.62	7.66	10.33	9.58	1 742
40 - 60	-17.31	-17.31	-17.40	-17.26	5.82	5.85	8.10	7.39	2 653
60 - 90	-17.95	-17.95	-17.97	-17.92	5.89	5.91	7.67	7.29	2 447

and non-differenced post-fit residuals estimated directly in their study.

The absolute SDEV values and biases from the first two periods are also comparable with the results from Bender et al. (2008). This result denotes a comparable quality of the double-difference-based processing with residuals converted to undifferenced ones using additional zero-mean conditions with the PPP results providing directly undifferenced residuals.

Tables 4 to 7 show the dependence of the SWD comparisons on the elevation. It must be kept in mind that these SWDs are not mapped back to the zenith, as in the comparison in Table 3. Both biases and standard deviations are significantly reduced with decreasing elevation angle, which corresponds to the length of the GPS signal propagation through the low atmosphere. Unfortunately, the lowest part of the atmosphere is crucial for the GPS tomography reconstruction because it crosses more voxels and contains more information about the water vapour content. It can be seen from the tables that the bias gradually decreases until 40° of elevation and then remains highly stable or increases slightly again. The same situation occurs for the SDEV, but with a change at an elevation of 30°. In June-July and October, the above-mentioned problems with WVR

measurement quality are clearly visible from the results biased up to 49 mm at the lowest elevations.

CONCLUSION

The results presented here indicate a high correlation between the slant wet delays derived from GPS using double-differencing and water vapour radiometer measurements. Adding the post-fit residuals to the GPS SWD had only a very small positive impact on bias, while it negatively influenced the standard deviation. The situation slightly improved after using the stacking maps for removing the multipath effect from the residuals. The results show that the post-fit residuals, even after multipath elimination, do not represent only the anisotropic part of the water vapour distribution but represent further insufficiencies in the model. Based on our results, we would therefore not recommend adding the post-fit residuals to SWD, at least with standard models currently used in Bernese GPS software. Generally, we obtained the best agreement between the GPS SWDs and WVR data-derived SWDs when the former were computed only from ZWD without any further investigation of horizontal gradients or residuals.

ACKNOWLEDGEMENT

This study was financed from the project of the Students´ Grant Competition n. SP/2011104 at VŠB-Technical University of Ostrava and partly supported by the Czech Science Foundation (No. P209/12/2207). Data acquisition of the Water Vapour Radiometer and GOPE GNSS station are supported by the project of large research infrastructure CzechGeo/EPOS (Project No LM2010008) and the Ministry of Education, Youth and Sports (Project No LC506).

REFERENCES

Alber, C., Ware, R.H., Rocken, C. and Braun, J.J.: 2000, Inverting GPS double differences to obtain single path phase delays. Geophysical Research Letters, 27, 2661–2664.

Bender, M., Dick, G., Ge, M., Deng, Z., Wickert, J., Kahle, H.-G., Raabe, A. and Tetzlaff, G.: 2011, Development of a GNSS water vapour tomography system using algebraic reconstruction techniques, Advances in Space Research, 47, Issue 10, 1704–1720.

Bevis, M., Businger, S., Herring, T.A., Rocken, C., Anthes, R.A. and Ware, R.H.: 1992, GPS meteorology – remote-sensing of atmospheric water-vapor using the global positioning system. Journal of Geohysical Research-Atmospheres, 97, Issue D14, 15787–15801.

Bevis, M., Chiswell, S., Hering, T. A., Anthes, R., Rocken, C. and Ware, R.H.: 1994, GPS Meteorology: Mapping zenith wet delays onto precipitable water, Journal of Applied Meteorology, 33, 379–386.

Boehm, J., Werl, B. and Schuh, H.: 2006, Troposphere mapping functions for GPS and very long baseline interferometry from European Centre for Medium-Range Weather Forecasts operational analysis data, Journal of Geophysicial Research, 111, B02406, doi:10.1029/2005JB003629.

Boehm, J. and Schuh, H.: 2007, Troposphere gradients from the ECMWF in VLBI analysis, Journal of Geodesy, doi:10.1007/s00190-007-0144-2

Byram, S.: 2011, IGS Final Troposphere product transition to USNO [IGSMAIL-6443].

Champollion, C., Masson, F., Bouin, M.-N., Walpersdorf, A., Doerflinger, E., Bock, O. and Van Baelen, J.: 2004, GPS water vapour tomography: preliminary results from the ESCOMPTE field experiment, Atmospheric research, 74, 253–274.

Dach, R., Hugentobler, U., Fridez, P. and Meindl, M.: 2007, GPS Bernese Software, Version 5.0, Astronomical Institute, University of Berne, Berne.

Duan, J., Bevis, M., Fang, P., Bock, Y., Chiswell, S., Businger, S., Rocken, C., Solheim, F., van Hove, T., Ware, R., McClusky, S., Herring, T. and King, R.: 1996, GPS meteorology: Direct estimation of the absolute value of precipitable water. Journal Appl. M., 24(24), 830–838.

Elosegui, P. and Davis, J.L.: 2003, Accuracy assessment of GPS slant-path determinations. GPS Meteorology: Ground-Based and Space-Borne Applications Workshop, Tsukuba, Japan, January 14–17.

Flores, A., Rius, A., Vilá-Guearou, J. and Escudero, A.: 2001, Spatio-temporal tomography of the lower troposphere using GPS signals, Phys. Chem. Earth (A), 26, No. 6-8, 405–411.

Gradinarsky, L.P. and Jarlemark, P.: 2004, Ground-based GPS tomography of water vapor: Analysis of simulated and real data, Journal of the Meteorological Society of Japan, 82, No. 1B, 551–560.

Niell, A.E.: 1996, Global mapping functions for the atmospheric delay at radio wavelengths, Journal of Geophysical Research, 101, 3227–3246.

Nilsson, T., Gradinarsky, L. and Elgered, G.: 2005, Assessment of tomographic methods for estimation of atmospheric water vapour using ground-based GPS, Chalmers University of Technology, Göteborg, Sweeden.

Noguchi, W., Yoshihara, T., Tsuda, T. and Hirahara, K.: 2004, Time-height distribution of water vapor derived by moving cell tomography during Tsukuba GPS campaigns, Journal of the Meteorological Society of Japan, 82, No. 1B, 561–568.

Saastamoinen, I.I.: 1973, Contribution to the theory of atmospheric refraction, Bulletin Géodésique, 107, 13–33.

Sever, Y.B.: 2010, Reprocesed IGS tropo product now available with gradients [IGSMAIL-6298].

Shoji, J. Nakamura, H., Iwabuchi, T., Aonashi, K., Seko, H., Mishima, K., Itagaki, A., Ichikawa, R. and Ohtani, R.: 2004, Tsukuba GPS dense net campaign observation: Improvement in GPS analysis of slant path delay by stacking one-way postfit phase residuals, Journal of the Meteorological Society of Japan, 82, No. 1B, 301–314.

Troller, M., Geiger, A., Brockmann, E., Bettems, J.M., Burki, B. and Kahle, H.G.: 2006, Tomographic determination of the spatial distribution of water vapor using GPS observations, Advances in Space Research, No. 37, 2211–2217.

Ware, R., Alber C., Rocken, C. and Solheim, F.: 1997, Sensing integrated water vapour along GPS ray paths, Geophysical Research Letters, 24, 417–420.

Zumberge, J.F., Heflin, M.B., Jefferson, D.C., Watkins, M.M. and Webb, F.H.: 1997, Precise Point Positioning for the efficient and robust analysis of GPS data from large networks, Journal of Geophysical Research, 102(B3), 5005–5017.

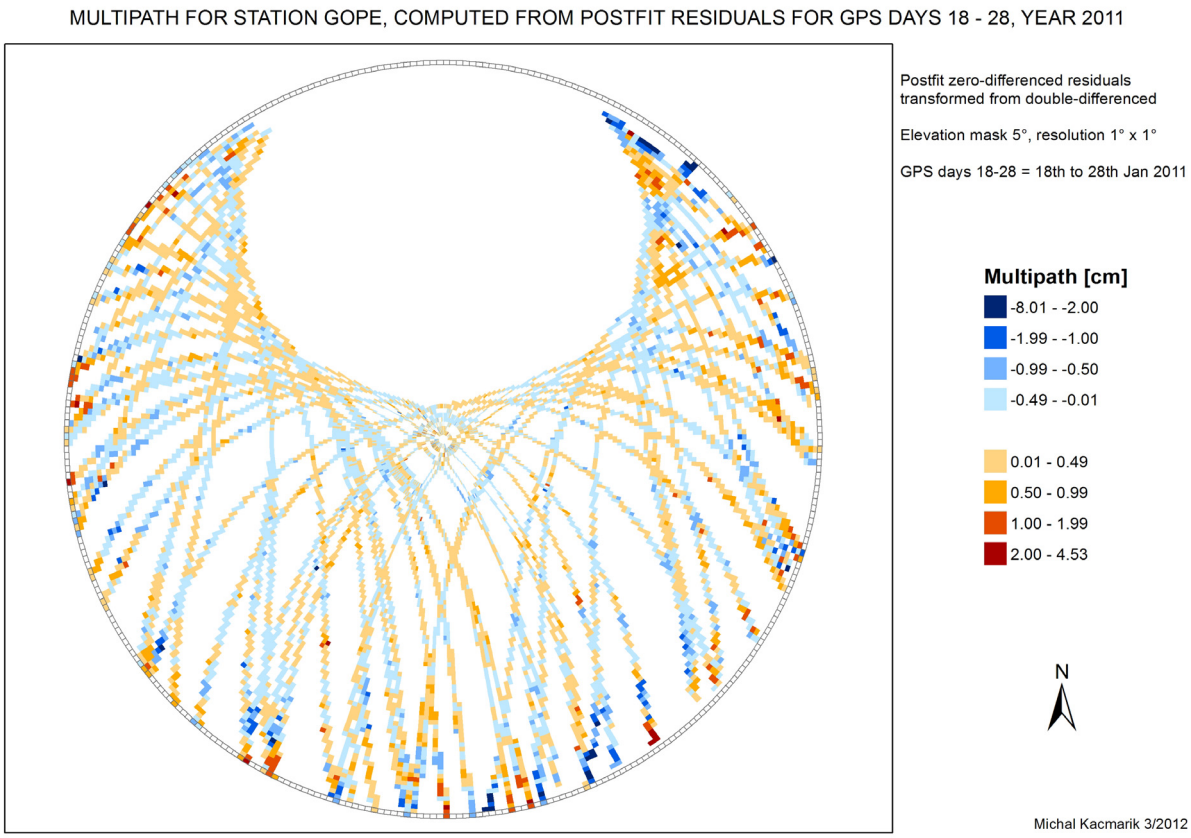

Fig. 1 Multipath stacking map for station GOPE, computed from GPS days 18 – 28, year 2011.

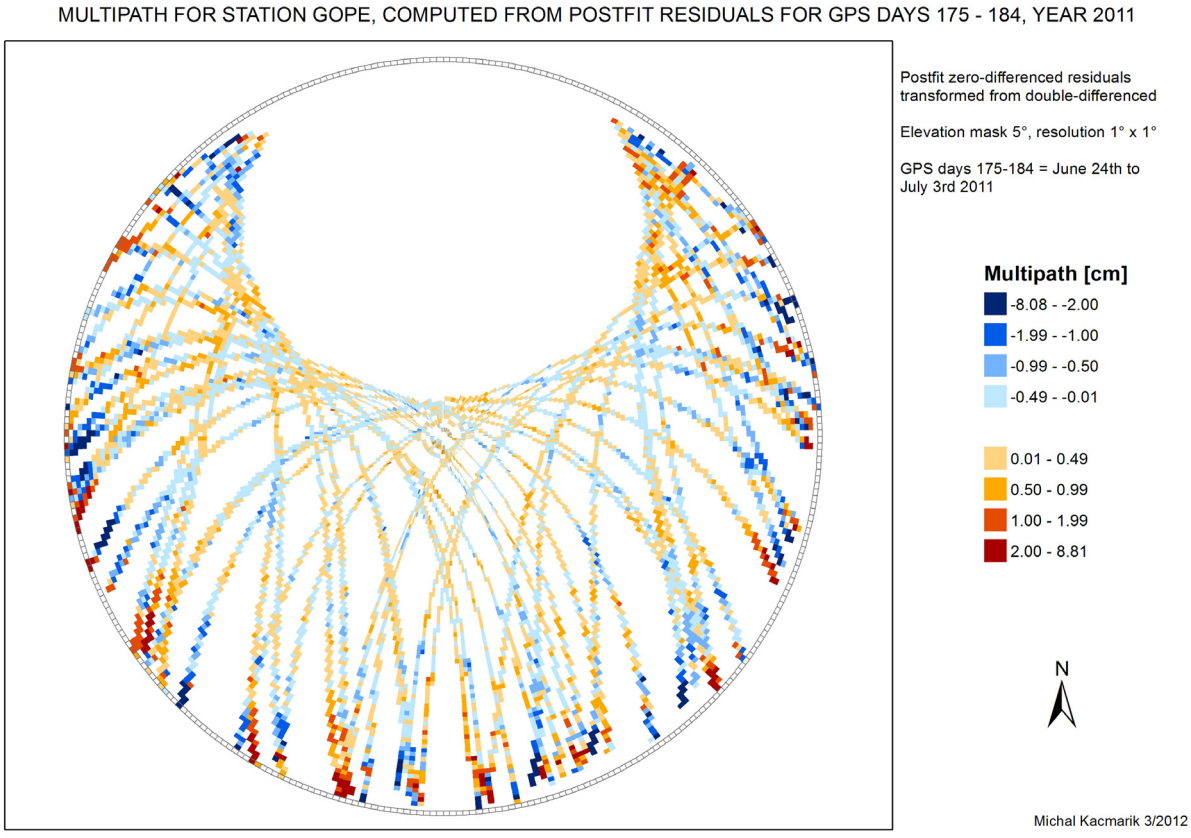

Fig. 2 Multipath stacking map for station GOPE, computed from GPS days 175 – 184, year 2011.